RoomTemperature, HighSNR Upconversion Spectrometer in the 6–12 µm Region.

Rodrigo, Peter John; Høgstedt, Lasse; Friis, Søren Michael Mørk; Lindvold, Lars René; Tidemand-Lichtenberg, Peter; Pedersen, Christian

Published in:
Laser & Photonics Reviews

Link to article, DOI:
10.1002/lpor.202000443

Publication date:
2021

Document Version
Peer reviewed version

Laser & Photonics Reviews

Room-temperature, high-SNR upconversion spectrometer in the 6-12 μm region

--Manuscript Draft--

Manuscript Number:	
Article Type:	Original Paper
Corresponding Author:	Peter John Rodrigo, Ph.D. Technical University of Denmark Department of Photonic Engineering: Danmarks Tekniske Universitet Institut for Fotonik Roskilde, DENMARK DENMARK
Corresponding Author E-Mail:	pejr@fotonik.dtu.dk
Order of Authors:	Peter John Rodrigo
	Lasse Høgstedt
	Søren Michael Mørk Friis
	Lars René Lindvold
	Peter Tidemand-Lichtenberg
	Christian Pedersen
Keywords:	upconversion; nonlinear optics; sum-frequency generation; mid-infrared spectroscopy; Fourier transform infrared spectrometer
Section/Category:	
Abstract:	Mid-infrared (MIR) spectroscopy, which has important applications in medicine, environmental monitoring, materials and food science, is widely performed using Fourier transform infrared (FTIR) spectrometers as gold standard. Despite decades of development, FTIR systems are vulnerable to vibration and have limited temporal resolution due to reliance on mechanically scanned mirrors and MIR direct detectors that have slower response than their near-infrared counterparts. Using cryogenically cooled detectors, state-of-the-art FTIR systems have reached a signal-to-noise ratio (SNR) of ~6,000 at 1 s integration time (at 4 cm-1 spectral resolution). Here, a novel MIR upconversion spectrometer (MIRUS) is presented with a record-high SNR > 10,000 at 1 s (6 cm-1 resolution), outperforming FTIR systems by circumventing the need for sophisticated cooling and any moving part, thus enabling operation in harsh environment. It has a spectral coverage of 6-12 μm – the broadest for an upconversion spectrometer to date. The MIRUS uses broadband intracavity upconversion to convert the signal spanning the MIR fingerprint region to the near-infrared where sensitive Si-detector based spectrometers operate with rates easily reaching kilospectra s–1. Applications of MIRUS for gas sensing, plastic identification and rapid photopolymerization monitoring are demonstrated.
Suggested Reviewers:	Juan Capmany Miguel Hernandez University of Elche: Universidad Miguel Hernandez de Elche jcapmany@umh.es
	Haim Suchowski Tel Aviv University Raymond and Beverly Sackler Faculty of Exact Sciences haimsu@tauex.tau.ac.il
Opposed Reviewers:	
Author Comments:	
Additional Information:	
Question	**Response**
Please submit a plain text version of your cover letter here.	8 October 2020 Dear Editor(s) of Laser & Photonics Reviews,

	We would like to submit our article with title “Room-temperature, high-SNR upconversion spectrometer in the 6-12 μm region” for your consideration in Laser & Photonics Reviews (LPR). As a promising alternative to Fourier Transform Infrared (FTIR) spectrometers that heavily rely on cryogenically cooled detectors, we demonstrate a mid-infrared upconversion spectrometer (MIRUS) that features room-temperature operation, record-high signal-to-noise ratio (>10,000 at 1 second spectral sampling time), no moving parts, and spectral coverage spanning 6 – 12 μm of the spectral fingerprint region. To our knowledge, this is the broadest spectral coverage achieved by an upconversion spectrometer thus far. In this Article, we present a novel upconversion spectrometer based on stacked AgGaS2 nonlinear crystals with different cut angles that enables MIRUS to achieve the abovementioned features. Furthermore, we highlight the utility of the MIR upconversion spectrometer by demonstrating a few example applications including gas spectroscopy, plastic identification, and real-time monitoring of the kinetics of fast-curing photopolymers. We believe that MIRUS, having advantages over the present gold standard (i.e., FTIR), can open doors in many other applications where fast chemical kinetics can be probed by means of spectroscopy in the MIR fingerprint region. All authors have contributed to the manuscript and agree with its submission to LPR. The work has not been published or submitted (either completely or in part, or in any other form or language) for publication elsewhere. In the manuscript, we also include a conflict of interest declaration. Yours sincerely, Peter John Rodrigo Corresponding Author DTU Fotonik Department of Photonics Engineering Technical University of Denmark Frederiksborgvej 399 4000 Roskilde Denmark E-mail: pejr@fotonik.dtu.dk
Do you or any of your co-authors have a conflict of interest to declare?	Yes
Please state: as follow-up to "Do you or any of your co-authors have a conflict of interest to declare?"	L. Høgstedt and S. M. M. Friis represent the company NLIR that also produces and sells infrared measurement equipment similar to the prototype used in this paper. P. Tidemand-Lichtenberg and C. Pedersen work at DTU Fotonik but are also part of the founding team of NLIR, each having a smaller share of the company. P. J. Rodrigo and L. R. Linvold declare no conflict of interest.

WILEY-VCH

Room-temperature, high-SNR upconversion spectrometer in the 6-12 µm region

Peter John Rodrigo, Lasse Høgstedt, Søren Michael Mørk Friis, Lars René Lindvold, Peter Tidemand-Lichtenberg and Christian Pedersen*

P. J. Rodrigo
DTU Fotonik, Technical University of Denmark, Frederiksborgvej 399, 4000 Roskilde, Denmark
E-mail: pejr@fotonik.dtu.dk

L. Høgstedt, S. M. M. Friis
NLIR ApS, Hirsemarken 1, 3520 Farum, Denmark

L. R. Linvold
DTU Health Tech, Technical University of Denmark, Frederiksborgvej 399, 4000 Roskilde, Denmark

P. Tidemand-Lichtenberg and C. Pedersen
DTU Fotonik, Technical University of Denmark, Frederiksborgvej 399, 4000 Roskilde, Denmark

Keywords: upconversion, nonlinear optics, sum-frequency generation, mid-infrared spectroscopy, Fourier transform infrared spectrometer

Mid-infrared (MIR) spectroscopy, which has important applications in medicine, environmental monitoring, materials and food science, is widely performed using Fourier transform infrared (FTIR) spectrometers as gold standard. Despite decades of development, FTIR systems are vulnerable to vibration and have limited temporal resolution due to reliance on mechanically scanned mirrors and MIR direct detectors that have slower response than their near-infrared counterparts. Using cryogenically cooled detectors, state-of-the-art FTIR systems have reached a signal-to-noise ratio (SNR) of ~6,000 at 1 s integration time (at 4 cm^{-1} spectral resolution). Here, a novel MIR upconversion spectrometer (MIRUS) is presented with a record-high SNR > 10,000 at 1 s (6 cm^{-1} resolution), outperforming FTIR systems by circumventing the need for sophisticated cooling and any moving part, thus enabling operation in harsh environment. It has a spectral coverage of 6-12 µm – the broadest for an upconversion spectrometer to date. The MIRUS uses broadband intracavity upconversion to convert the signal spanning the MIR fingerprint region to the near-infrared where sensitive Si-

detector based spectrometers operate with rates easily reaching kilospectra s^{-1}. Applications of MIRUS for gas sensing, plastic identification and rapid photopolymerization monitoring are demonstrated.

1. Introduction

The importance of mid-infrared (MIR) spectroscopy in many scientific and applied fields is evident as it enables access to the spectral fingerprint region (~ 6-12 µm). Since most molecules have rotational-vibrational transitions that strongly manifest in this spectral regime, MIR spectroscopy provides for a simple and sensitive means to probe various materials in gas, liquid or solid phases with high chemical specificity. Conventional Fourier transform infrared (FTIR) spectrometers have been the instrument of choice for most MIR spectroscopy applications[1]. This can be attributed to the fact that FTIR systems provide ultra-broadband spectral coverage but also relatively high spectral resolution. FTIR based MIR spectroscopy has become a powerful analytical tool in biomedical fields[2,3], materials[4] and environmental[5] sciences, and food analyses[6,7]. Despite their widespread use, conventional FTIR spectrometers have disadvantages. For example, the need to mechanically scan a mirror and cryogenically cool the detectors limits the measurement speed, ruggedness, operational complexity and cost-effectiveness of FTIR systems. High signal-to-noise ratio (SNR) combined with high temporal resolution are essential in a number of MIR spectroscopy applications such as the quantitative, time-resolved monitoring of photopolymerization processes[8,9].

Other technologies have been introduced to circumvent some of the drawbacks associated with conventional FTIR systems. FTIR systems with fixed components have been realized by exploiting interferograms produced in the spatial rather than in time domain[10–13]. These new FTIR (spatial type) systems have improved mechanical stability but have the same

major drawback as the conventional FTIR (temporal type) in terms of the necessity of using cryogenically cooled MIR detectors to achieve a practical SNR performance or measurement speed. A novel technology that is emerging as a strong alternative to both types of FTIR systems is the MIR upconversion spectrometer (MIRUS)[14–22]. In MIRUS, the MIR signal is converted to the shorter near-infrared (NIR) as a result of a generalized sum-frequency generation (SFG) process[23,24] with a high-power pump laser (e.g., at 1 μm) inside a nonlinear crystal. The generalization is based on the extension of SFG beyond the scalar phase-matching[25] to a vectorial phase-matching condition[23,24]. This enables access to noncollinear interaction of input and pump fields allowing simultaneous upconversion of MIR signals – enabling broad spectral coverage. The resulting upconverted signal can then be analyzed spectrally using a silicon (Si) based spectrometer that is nearly background-noise-free and does not require cryogenic cooling. The measurement speed is not limited by the upconversion process but rather by the NIR detector bandwidth and/or sensitivity. This feature has recently enabled the realization of time-resolved upconversion spectroscopy in the 2.2-2.4 μm region with a temporal response of 75 ps[19]. The efficient translation of the MIR spectrum to the NIR is key to the success of MIRUS, since MIR detectors (e.g., HgCdTe) used in FTIR spectrometers suffer from intrinsic thermal background noise, lower detectivity and slower response compared to their NIR counterparts. MIR noise from thermal emission of the nonlinear crystal itself is minimal due to the high transparency of the nonlinear material. MIRUS is based on a second-order nonlinear frequency conversion process followed by NIR detection – in strong contrast to direct MIR detection. When crystal absorption is absent in the wavelength range of interest, so is the thermal blackbody radiation[26], effectively eliminating fundamental thermal radiation noise that hampers direct MIR detectors operating at room temperatures. When photons are spectrally translated from MIR to NIR, the bandgap of NIR detectors is well above the energy level of room-temperature Planck radiation, thus allowing MIRUS to operate at room temperature with low noise. Previous MIRUS implementations

based on periodic-poled lithium niobate (PPLN)[14,15], chirped-poled lithium niobate (CPLN)[16,17] and fanout quasi-phase-matched lithium niobate[18,19] have covered the wavelength range (or sub-ranges) between 2 µm and 5 µm. High conversion efficiency in these systems was achieved by using intracavity laser pumping scheme. The upper limit of the spectral coverage of PPLN-based MIRUS is ultimately restricted by the transparency window of lithium niobate ($LiNbO_4$), which strongly absorbs at wavelengths greater than 5.3 µm. MIRUS designs that cover longer wavelengths (> 5 µm) have therefore used other nonlinear crystals, such as $LiInS_2$[20] and $AgGaS_2$[21,22]. These designs are non-ideal in terms of achieving a high-SNR spectrometer in the 6-12 µm range. Firstly, intracavity designs using $AgGaS_2$ are very challenging due to significant thermal lensing (as short as 20 mm focal length), caused by partial absorption of the high-power upconversion pump laser in the $AgGaS_2$ crystal. Thermal lensing easily causes instability in the circulating pump field resulting in a decreased SNR of the system. A 6.1-6.8 µm system based on $AgGaS_2$ has been demonstrated[21]. To overcome thermal lensing, a system using $LiInS_2$ was attempted, with its better thermal properties, however, strong MIR absorption in $LiInS_2$ prevents usage beyond 9 µm[20]. A single-pass design, i.e., avoiding the intracavity complexity, used multiple pump sources to achieve broadband upconversion in $AgGaS_2$, however, the sophistication of using multiple pumps made this design impractical and the SNR is far inferior to intracavity designs[22]. Nevertheless, challenges and insights encountered in these early attempts have pushed the MIRUS technology forward and led to this work.

In this work, we present a new design to achieve, to our best knowledge, the widest spectral coverage in the MIR fingerprint region (6-12 µm) and a record peak SNR (> 10,000 at 1 s) for an upconversion spectrometer to date. The record-high spectral coverage is obtained by combining noncollinear upconversion and the use of multiple nonlinear $AgGaS_2$ crystals with different cut angles. The high SNR is a result of a design where the $AgGaS_2$ crystals are implemented as intracavity components in a high-finesse 1064 nm laser cavity –

hereby, ensuring high upconversion efficiency. In contrast to FTIR systems, the new MIRUS employs an uncooled Si detector and all components are stationary. Design considerations for the ultra-broadband MIRUS such as $AgGaS_2$ cut angles, phase-match curves and performance simulations comparing one-, two- and three-crystal architectures, and SNR characterization are also discussed. Subsequently, applications of the upconversion spectrometer are demonstrated for fast spectral characterization of different samples including plastics, gases, and liquid photopolymer samples that are solidified (cured) by exposure to UV radiation. Finally, we compare the performance parameters of the 6-12 µm MIRUS and the two types of FTIR systems and give some concluding remarks including outlook for future work.

2. Principles of 6-12 µm upconversion spectrometer

A schematic diagram and a photograph of the MIRUS are shown in **Figure 1a** and **Figure 1b**, respectively. The system consists of three modular parts: a collimated broadband MIR source, an upconversion module, and a NIR grating spectrometer. The MIR source is a silicon nitride (SiN) globar (Model IR-Si272, Scitec Instruments Ltd.) positioned near the focal point of a 25 mm diameter parabolic reflector. The upconversion module consists of a 1064 nm Nd:YVO_4 (folded) laser cavity inserted with a series of three (or two) anti-reflection (AR) coated $AgGaS_2$ crystals. The NIR spectrometer employs a Si-based back-thinned CCD 2048-pixel linear array detector (Hamamatsu Photonics) operating at room temperature. The nonlinear crystals are intracavity in order to access the highest available pump power to achieve high upconversion efficiency[23,24]. In contrast to the multi-pump scheme that relied on single-pass pump lasers with powers in the order of 0.1 W[22], the 6-12 µm MIRUS achieves a circulating pump power two orders of magnitude larger (~20 W). This is estimated from the measured 1064 nm leakage power out of the laser cavity mirror M1, multiplied by the factor $(1 - R)^{-1}$, where R is the reflectance of the mirror surface with high-reflection coating at 1064 nm. The

globar spectrum can be modeled as the emission spectrum of a blackbody at temperature of 1173 K. Open-path transmission spectroscopy is readily performed by introducing the sample (e.g., plastics and gases) in the gap of a few centimeters between the MIR source and the upconversion module. For the experiments demonstrating real-time monitoring of photopolymerization, an attenuated total reflection (ATR) module that employs a ZnSe sample substrate is inserted between these modules (see Materials and methods). The 25 mm input aperture of the upconversion module is an AR-coated plano-convex Ge lens (L1; focal length f = 12.5 mm) that focuses the MIR signal into the $AgGaS_2$ crystals. The MIR signal is mixed with the 1064 nm intracavity pump beam inside the $AgGaS_2$ crystals – resulting in an upconverted light in the NIR region (900-980 nm) through Type-II SFG. With an intracavity lens L2, the pump beam waist radius, at exp(–2) intensity, inside the $AgGaS_2$ crystals is 120 µm. The upconverted light couples into the NIR spectrometer via a collimating lens L3. The MIR spectrum is calculated from the NIR spectrum using the energy conservation relation $\lambda_{up}^{-1} = \lambda_{MIR}^{-1} + \lambda_{pump}^{-1}$ where λ_{up}, λ_{MIR} and λ_{pump} are the wavelengths of the upconverted signal, MIR signal and pump beam, respectively.

The broad spectral coverage of MIRUS without any parametric tuning (i.e., without need for mechanical movement of a nonlinear crystal and/or varying of pump wavelength) is achieved by combining collinear and noncollinear phase-matching in a series of $AgGaS_2$ crystals with different cut angles (**Figure 2a**). To understand this proposed scheme, a numerical simulation of the upconverted signal was performed based on one, two and three $AgGaS_2$ crystals. A collimated beam with broad MIR spectrum is incident on the focusing lens L1 in **Figure 2a**. The optical field for each wavelength component λ_{MIR} can be described by a superposition of plane waves inside the $AgGaS_2$ crystal(s) with different internal input angle θ_{MIR} measured relative to the 1064 nm pump propagation axis. For each λ_{MIR}, energy conservation defines the wavelength λ_{up} of the upconverted field E_{up} and phase-matching requirement for a given crystal cut angle means that conversion efficiency only depends on

θ_{MIR}. Consequently, the upconverted beam power P_{up} at λ_{up} can be obtained by integrating the upconverted intensity, which depends on the far-field output angle, defined as $z_f^{-1}(x^2 + y^2)^{1/2}$ in **Figure 2a** where (x, y) are the coordinates in the observation plane at a far-field distance z_f. Using a theoretical model of the upconversion process for a Gaussian pump beam with power P_{pump} and beam radius w_0 inside a nonlinear crystal[23], the upconverted signal power P_{up} for each λ_{up} (corresponding to each λ_{MIR} from 5 µm to 13 µm in steps of 0.25 µm) is calculated using:

$$P_{up} = \frac{cn_{up}\varepsilon_0}{2}\iint |E_{up}|^2 \,dxdy = \frac{P_{pump}}{z_f^2}\frac{w_0^2 d_{eff}^2\, \omega_{up}^4\, L^2}{\pi\varepsilon_0 c^5}\cdot I_{MIR}\cdot \mathrm{sinc}^2\left(\frac{\Delta k_z L}{2}\right)\cdot\iint \exp\left(-\frac{\Delta k_T^2 w_0^2}{2}\right)dxdy, \quad (1)$$

where Δk_z and Δk_T are the longitudinal and transverse components of the phase mismatch, respectively. For multiple $AgGaS_2$ crystals, P_{up} is calculated for each crystal and then summed up. The nonlinear coefficient and length of the $AgGaS_2$ crystal are denoted by d_{eff} and L, respectively. n_{up} and ω_{up} are the refractive index at λ_{up} and the angular frequency of the upconverted field, respectively, while I_{MIR} is the MIR signal intensity that depends on θ_{MIR} and λ_{MIR} according to the globar blackbody spectrum. First, the phase-match condition is considered in order to calculate Δk_z and Δk_T. To simplify the calculation of P_{up}, circular symmetry is considered, which allows the transformation of the integral in **Equation 1** into polar coordinates. This is a reasonable approximation since the change in $AgGaS_2$ refractive index with angle contributes very little to the phase mismatch (see Supplementary Information **Figure S1**). The phase-match curves for $AgGaS_2$ crystals with cut angles θ = 52.6°, θ = 45.6°, and θ = 42.8° are shown in **Figure 2b**. For each crystal, the corresponding phase-match curve indicates the internal input angle θ_{MIR} that optimizes the upconversion efficiency for a particular λ_{MIR}. For an $AgGaS_2$ crystal with a cut angle of θ = 52.6°, the optimal θ_{MIR} for 9 µm is about 16° (**Figure 2a**). With a refractive index of 2.3 for $AgGaS_2$, an external input angle of ~40° is required for 9 µm. This means that with a 25 mm diameter collimated MIR source, the MIR light needs to be focused by a lens (L1) with f ≤ 15 mm to

ensure spectral coverage of wavelengths spanning from 6 µm to 9 µm. Such wide MIR light feeding angle is represented by the first (Focusing 1) in three types of MIR focusing geometries shown in **Figure 2c**. However, the upconversion efficiency decreases from collinear to noncollinear interaction between MIR signal and the pump[23,21]. Consequently, the upconverted power for a single $AgGaS_2$ crystal based MIRUS suffers from a substantial roll-off for increasing λ_{MIR} as shown in **Figure 2d**. The degree of roll-off also depends on the chosen MIR focusing geometry. The three focusing geometries assume the MIR signal intensity to vary with θ_{MIR} according to $I(\theta_{MIR}) = I_0\exp[-(\theta_{MIR}/\theta_0)^4]$, where Focusing 1, 2, and 3 correspond to $\theta_0 = 20°$; $I_0 = 0.252$, $\theta_0 = 15°$; $I_0 = 0.446$, and $\theta_0 = 10°$; $I_0 = 1$, respectively, so the curves in **Figure 2c** appear normalized in optical power. The intensity profile is mathematically modelled to represent a distribution that gradually tailors off at the edges but is flat in the center. In the newly proposed MIRUS, the roll-off problem is addressed by the use of two-stack (length $L = 5$ mm each) or three-stack ($L = 3$ mm, $L = 3$ mm and $L = 4$ mm) $AgGaS_2$ crystals with a 5 x 5 mm^2 aperture size. The use of a series of $AgGaS_2$ crystals has two benefits. First, it reduces the roll-off problem inherent in single nonlinear crystal MIRUS and secondly, it reduces the need for a large feeding angle. The combination of these benefits results in a MIRUS with an ultra-wide spectral coverage from 5.7 µm to 12 µm (830 cm^{-1} to 1750 cm^{-1}) as shown in **Figure 2e** and verified experimentally in **Figure 3a**. The model shows good agreement with the experiment – in particular, it predicts the collinearly phase-matched λ_{MIR} (around 6 µm, 7.5 µm and 8.5 µm for the three-stack case) where steep gradients in the upconverted power occur. However, discrepancies occur between model and experimental data, for example, in the relative strengths of the peaks in **Figure 2e** and **Figure 3a** around the collinearly phase-matched λ_{MIR}. This is likely due to the fact that the present model does not include insertion losses through the $AgGaS_2$ crystals due to absorption and imperfect AR-coating of their surfaces. Furthermore, the exact spectral response of the upconversion module depends strongly on the exact alignment of the MIR input, e.g., longer

wavelengths can be favored by a slight tilt of the input. In the three-stack case, the $AgGaS_2$ crystal ($\theta = 42.8°$) that efficiently upconverts the longest MIR wavelengths is closest to the input aperture lens L1 while the crystal ($\theta = 52.6°$) for the shortest MIR wavelengths is farthest. This arrangement is selected in order to upconvert the longer MIR wavelengths (8.5-12 µm) in the first crystal avoiding severe absorption by a larger thickness of $AgGaS_2$. Although the shorter MIR wavelengths (6-8.5 µm) are absorbed less by $AgGaS_2$, they suffer from higher reflection losses due to the need to transmit through more interfaces to reach the second and third crystal before getting upconverted.

Although narrower in coverage than state-of-the-art FTIR systems, the proposed MIRUS has a compact footprint (27 x 17 x 9 cm^3), does not require cryogenic cooling and has no moving parts – features that could prove advantageous for many industrial applications such as in-line production monitoring where advanced laboratory equipment (e.g., vibration isolation, optical tables and cryogenic cooling systems) are not readily accessible. Furthermore, the MIRUS simultaneously probes all spectral bins in the 6-12 µm region at integration times down to 11 ms and has a measured SNR of > 10,000 at 1 s integration time as shown in **Figure 3b**. Here, SNR is defined as the ratio of the mean to the standard deviation of the globar spectrum measured by MIRUS. Our present spectral update rate is limited by the CCD linear array data readout speed and not by the sensitivity of the system. For some applications, a fast CMOS camera could be used as NIR detector[15] in MIRUS to achieve update rates in the order of 1000 spectra s^{-1}.

3. Applications of MIR upconversion spectrometer

3.1. Validation of MIRUS for spectroscopy of plastics and gases

We tested the utility of the 6-12 µm MIRUS for obtaining the MIR transmission spectra of various plastic sheets and gas species. The experimental setups for these demonstrations are

shown in **Figure 4a**. The spectra of polystyrene, tedlar and teflon sheets obtained using MIRUS are shown in **Figure 4b**. It can be seen that these three materials have distinguishable MIR spectra – demonstrating the potential application of the MIRUS technology for plastic identification or monitoring of multilayer plastic film production. The transmission spectrum of polystyrene shown in **Figure 4b** has many absorption lines, which we used to calibrate the wavelength (or wavenumber) axis of the MIRUS. The MIRUS spectra, taken at 11 ms integration time, are found to agree well with the spectra obtained by a conventional (scanning mirror based) FTIR spectrometer (Spectrum 100, Perkin Elmer) set to a spectral acquisition time of a few seconds and a spectral resolution of 8 cm^{-1}. In order to determine the spectral resolution of the MIRUS system, the collimated beam from the globar was replaced with the beam from a DFB-QCL (QD7950CM1, Thorlabs) operating at 7.94 µm (1259 cm^{-1}; linewidth = 0.25 cm^{-1}) or a widely tunable QCL (Mini-QCL-100, Block Engineering) operating in the range 9.3 µm to 12 µm (830 cm^{-1} to 1070 cm^{-1}; linewidth = 1 cm^{-1} to 2 cm^{-1}). Based on the full-width-half-maximum (FWHM) of individual spectral peaks in **Figure S2**, also listed in **Table S1** (see Supplementary Information), the measured spectral resolution of the present MIRUS is better than 6 cm^{-1}. The resolution is currently not limited by the linewidth of the 1064 nm pump (~0.35 nm; see **Figure S3**), which would account only for a 3 cm^{-1} broadening. In **Figure 4c** and **Figure 4d**, the MIR transmission spectra of two gas species, nitrous oxide (N_2O) and tetrafluoropropene ($C_3H_2F_4$), obtained by MIRUS are plotted and shown to agree well with corresponding reference data (HITRAN 2016 for N_2O and FTIR measurement for $C_3H_2F_4$ found elsewhere[27]). The two gases were individually introduced in the path of the collimated MIR beam in front of the upconversion module input aperture. Again, due to the spectral coverage of the MIRUS in the fingerprint region, the spectrometer demonstrates its capability for trace gas detection and identification. For such application, the setup could also include a gas cell between the globar and upconversion module for a more controlled and quantitative gas absorption spectroscopy.

3.2. Monitoring of fast photopolymerization kinetics using MIRUS

One example application where a high temporal resolution MIR spectrometer is highly attractive is photopolymerization. Accurate measurements of the kinetics of photopolymerization are of great interest both from a scientific point of view as well as for process optimization in industry[8,9]. Photopolymers play an important role in industrial and medical applications – from photocurable printing inks for flexoprinting[28], UV curable resins for car bodywork, dental fillings[29], medical devices[28,30] and 3D printing for tissue engineering[31,32]. **Figure 5** shows data obtained using the MIRUS technology for studying the fast kinetics of UV-cured photopolymers. In these experiments, an ATR accessory (see Materials and methods) is used with the MIRUS setup as shown in **Figure 5a**. After taking a reference spectrum (used for normalization), a drop (~1 ml) of the liquid monomer-oligomer-photoinitiator mixture is placed on the ZnSe ATR substrate (covering a round area of about 10 mm diameter). With the ATR, the spectrum measured using MIRUS represents the transmission spectrum of the probed layer of the sample adjacent to the ZnSe surface, with a total transmission path length determined by the product of the probing depth (~2 µm) and the number of reflections (about 10) on the ZnSe-sample interface. Transmission spectra are recorded at 11 ms integration time per spectrum a few seconds before and after a UV LED illumination source is switched on. The UV LED source has an operating wavelength of 385 nm emitted from a fiber tip placed 6 cm away from the sample (power density of 24 mW cm^{-2}). Five photopolymer samples with different photoinitiator concentrations were used to demonstrate the capability of the MIRUS to probe the dependence of curing rate on photoinitiator concentration.

The spectrum before UV irradiation is compared to a spectrum obtained 8 s after the UV LED was switched on (i.e., after curing) as depicted in **Figure 5b**. Two vertical dashed

lines indicate two main absorption lines at 1437 cm^{-1} and 1640 cm^{-1}, which are known to correspond to the twisting and stretching of alkene (C = C) functional group, respectively[33]. Note that the absorbance at these two wavenumbers decreases (more evidently at 1640 cm^{-1}) as the sample is cured by the UV irradiation. The ability of MIRUS to track the change in absorbance over time, with high temporal resolution, enables real-time monitoring of photopolymerization kinetics and accurate calculation of conversion rates. Using the method described by Decker[9], the degree of conversion p was calculated from the decrease in (integrated) absorbance A as a function of irradiation time t: $p = 1 - (A_t/A_0)$, where A_t is the absorbance at t and A_0 is the absorbance at the time when the UV LED source was switched on. Conversion p is calculated for the absorbance peak at 1640 cm^{-1}, integrated in a 30 cm^{-1} wide band.

Based on the real-time recording of the IR spectra in the fingerprint region (see **Movie V1** and Supplementary Information), two plots showing the kinetics of the photopolymerization have been produced (**Figure 5c** and **Figure 5d**). **Figure 5c** shows the progression of the photopolymerization process at different PI concentrations. From these curves it can be inferred that the photocuring process achieves the fastest rate when the photoinitiator (TPO) constitutes 5% w/v of the base monomer (HDDA). The results, furthermore, show that 2.5% w/v of photoinitiator achieves the same conversion $p = 0.5$ equal to full cure of the polymer. This type of information is useful for the design of photopolymer resins, as photoinitiators are by far the most expensive compound in a photopolymer resin. The fact that there is an optimum in the concentration of the photoinitiator can be attributed to the photopolymerization process. As it can be seen from the curves in **Figure 5c** and **Figure 5d**, the conversion of monomer and rate of conversion increase monotonically with increasing photoinitiator concentration from 0.1% to 2.5% w/v.

4. Discussion and outlook

It may be stated that the "holy grail" of spectroscopy is: a spectrometer with high SNR, fast measurement rate, high spectral resolution, wide spectral coverage, small form factor (i.e., lightweight), no cooling, and no scanning components. The MIRUS demonstrated in this work has the potential of achieving a good balance of these criteria. In **Table 1**, the two types of FTIR, both commercially available (see Supplementary Information for links to some specific representative instruments for each technology), are listed with their key performance parameters and compared to the 6-12 µm MIRUS presented in this work. At comparable spectral resolution settings (4 cm^{-1} for temporal or scanning-type FTIR and 6 cm^{-1} for MIRUS), the presented MIRUS has an SNR > 10,000 while a scanning-type FTIR with a liquid nitrogen (LN_2) cooled detector has an SNR of 6,000, both at 1 s integration or acquisition time. With an update rate of 40 spectra s^{-1}, MIRUS already outperforms the scanning-type FTIR but this rate can readily be improved to 1,000 spectra s^{-1} using Si-based CMOS detector[15]. MIR detectors are known to be limited in speed, which prevents FTIR systems from achieving kHz measurement rates. The present MIRUS spectral resolution of 5-6 cm^{-1}, which can still be improved, is also at par with that of commercial Sagnac interferometer based or spatial-type FTIR, which has the poorest SNR and measurement rate performance among the three globar-based spectrometer technologies. One factor that limits the spectral resolution of the Sagnac-type FTIR is the limited number of pixels available when using direct MIR detector arrays. Using a NIR spectrometer with an improved spectral resolution (e.g., based on Echelle grating) and an upconversion system based on a ring cavity configuration[34] (instead of the current standing-wave cavity) with a 1064 nm mixing laser operating in a single longitudinal mode (i.e., with linewidth much less than 0.1 nm), future MIRUS implementations could achieve a spectral resolution in the order of 1 cm^{-1}.

SNR improvements in MIRUS are also possible by increasing the 1064 nm circulating power available for the upconversion process. The currently estimated 20 W of 1064 nm intracavity power is limited by thermal lensing in the $AgGaS_2$ crystals and overall insertion losses experienced by the 1064 nm pump due to partial absorption in $AgGaS_2$ and imperfect AR-coating on the facets of the crystals. The insertion loss in commercially available $AgGaS_2$ still varies from crystal to crystal. Careful selection of crystals with the lowest insertion losses (not only at λ_{pump}, but also at λ_{MIR} and λ_{up}) will benefit future MIRUS implementations in terms of SNR performance. The use of a ring cavity system would also enable increased circulating 1064 nm pump power, as it would reduce the losses and the thermal load on the nonlinear crystals per cavity-roundtrip.

The new upconversion spectrometer proposed in this paper is particularly well suited for the study of fast kinetics of chemical reactions in photopolymers[8,9] as it provides speed and insensitivity to the light used to trigger the photochemical reaction. The spectral coverage spanning the fingerprint region allows MIRUS to simultaneously probe different functional groups or perform multispecies reaction kinetics in real time. As shown by our measurements of the spectra of two QCLs (**Figure S2**), the MIRUS can be used as an optical spectrum analyzer for routine characterization of MIR light sources (i.e., the globar is replaced by the source under test). Finally, the MIRUS demonstrated in this work can also serve as an analytical tool for a wide range of industrial applications in which FTIR is currently used such as monitoring of dairy products and wine[7], sugar[35,36], alcohol[37], and fermentation processes[38].

5. Materials and methods

5.1. Plastics and gases

As solid samples, we used thin sheets of polystyrene, tedlar and teflon. All plastic sheets were 0.1 mm thick and had an area larger than the cross-section of the collimated MIR source to ensure that all phase-match input angles and hence all MIR wavelengths between 6 µm to 12 µm pass through the sample. For the gas spectroscopy using MIRUS, a cartridge of N_2O gas (LISS) was used to spray laughing gas in the path of the illumination source; subsequently, tetrafluoropropene gas was sprayed in the beam path from an air duster (CA4-US, Thorlabs) typically used for cleaning optical components. To ensure that the gas was sufficiently spread over the cross-section of the collimated MIR source, the spray nozzle was positioned a few centimeters away from the optical axis.

5.2. ATR setup and photopolymer sample preparation

The ATR module (HATR, Perkin Elmer) employs a combination of two concave mirrors and two plane mirrors (all mirrors are aluminum-coated), and an ATR prism made of ZnSe (45 x 12 mm^2 sample area and 5 mm thick). The input and output apertures of the ATR setup have a diameter of 25 mm – matching the diameters of the collimated MIR beam from the SiN globar and the input Ge lens aperture of the MIRUS upconversion module.

To study the molecular changes of the monomer material in a photopolymerization process, a basic photopolymer material was made. This resin comprised a photoinitiator, Diphenyl(2,4,6-trimethylbenzoyl)phosphine oxide (TPO) from Sigma Aldrich 415952, 97% purity, and a monomer 1,6 Hexanediol diacrylate (HDDA) from Sigma Aldrich 246816, 80% purity. A stock resin containing 10% w/v of TPO in HDDA was made. The photopolymer resins with different PI concentrations were made by diluting the 10% stock resin solution

with HDDA to give the concentration values of 0.1%, 0.5%, 1%, 2.5% and 5% w/v of photoinitiator.

The choice of an acrylate monomer simply reflects the fact that acrylate based photopolymers are among the most ubiquitous photopolymers for industrial use. Furthermore, this photopolymer system is well described in the literature. All photopolymer samples on the ATR prism were covered with a transparent plastic sheet allowing the UV LED light to excite the photopolymer and prevent oxygen from inhibiting the photocuring process.

Acknowledgements
The authors acknowledge the financial support from the Eurostars MIRILUS project. The authors thank Magdalena Skowyra for technical assistance with the photopolymer samples, and Yu-pei Tseng and Mahmoud Tawfieq for assistance with the widely tunable QCL. C. P. came up with the idea of using stacked nonlinear crystals and was co-applicant of our Eurostars research grant. P. T. L. performed the numerical simulations. P. J. R. conducted the experiments demonstrating the performance and applications of MIRUS. L. H. and S. M. M. F. designed and assembled the MIRUS, and performed the SNR measurements. L. R. L. was responsible for the photopolymer sample preparation. P. J. R. and L. R. L. wrote the initial paper and all authors took part in the revision process.

Received: ((will be filled in by the editorial staff))
Revised: ((will be filled in by the editorial staff))
Published online: ((will be filled in by the editorial staff))

Conflict of interest
L. H. and S. M. M. F. represent the company NLIR that also produces and sells infrared measurement equipment similar to the prototype used in this paper. P. T. L. and C. P. work at DTU Fotonik but are also part of the founding team of NLIR, each having a smaller share of the company. P. J. R. and L. R. L. declare no conflict of interest.

References

[1] K. Gerwert, C. Kötting, "Fourier Transform Infrared (FTIR) Spectroscopy," in *Encyclopedia of Life Sciences*, John Wiley & Sons, New York, USA **2010**.

[2] M. Baker, J. Trevisan, P. Bassan, R. Bhargava, H. J. Butler, K. M. Dorling, P. R. Fielden, S. W. Fogarty, N. J. Fullwood, K. A. Heys, C. Hughes, P. Lasch, P. L. Martin-Hirsch, B. Obinaju, G. D. Sockalingum, J. Sulé-Suso, R. J. Strong, M. J. Walsh, B. R. Wood, P. Gardner, F. L. Martin. *Nat. Protoc.* **2014**, *9*, 1771.

[3] S. De Bruyne, M. M. Speeckaert, and J. R. Delanghe, *Crit. Rev. Clin. Lab. Sci.* **2018**, *55*, 1.

[4] L. B. Cimdina, N. Borodajenko, *Infrared Spectroscopy - Materials Science, Engineering and Technology*, (Ed: T. Theophanides), InTech, Rijeka, Croatia **2012**.

[5] C. M. Simonescu, "Applications of FTIR Spectroscopy in Environmental Studies," in *Advanced Aspects of Spectroscopy*, (Ed: M. A. Farrukh), IntechOpen, **2012**, Ch. 2. DOI: 10.5772/48331.

[6] Valand, R., Tanna, S., Lawson, G., Bengtström, L., *Food Addit. Contam. Part A* **2020**, 37, 19–38.

[7] S. K. Andersen, P. W. Hansen, H. V. Andersen, "Vibrational Spectroscopy in the Analysis of Dairy Products and Wine," in *Handbook of Vibrational Spectroscopy*, **2006** DOI:10.1002/0470027320.s6602.

[8] T. Scherzer, U. Decker, *Vib. Spectrosc.* **1999**, 19, 385–398.

[9] C. Decker, *Macromol. Rapid Commun.* **2002**, 23, 1067–1093.

[10] M. J. Padgett, A. R. Harvey, A. J. Duncan, W. and Sibbett, *Appl. Opt.* **1994**, 33, 6035–6040.

[11] P. Seitz, M. Stalder (Centre Suisse d'Electronique et de Microtechnique CSEM SA), *US 6222627B1*, **2001**.

[12] L. Xia, Z. Yang, S. Yin, Q. Deng, C. Du, *Opt. Eng.* **2014**, 53, 074109.

[13] M. Lenzner, J.-C. Diels, *Opt. Express* **2017**, 25, A447–A453.

[14] A. Barh, C. Pedersen, P. Tidemand-Lichtenberg, *Opt. Lett.* **2017**, 42, 1504–1507.

[15] S. Wolf, J. Kiessling, M. Kunz, G. Popko, K. Buse, F. Kühnemann, *Opt. Express* **2017**, 25, 14504–14515.

[16] S. M. M. Friis, L. Høgstedt, *Opt. Lett.* **2019**, 44, 4231–4234.

[17] K. E. Jahromi, Q. Pan, L. Høgstedt, S. M. M. Friis, A. Khodabakhsh, P. M. Moselund, F. J. M. Harren, *Opt. Express* **2019**, 27, 24469–24480.

[18] A. Barh, M. Tawfieq, B. Sumpf, C. Pedersen, P. Tidemand-Lichtenberg, *Opt. Lett.***2019**, 44, 2847–2850.

[19] B. Julsgaard, N. von den Driesch, P. Tidemand-Lichtenberg, C. Pedersen, Z. Ikonic, D. Buca, *Photon. Res.* **2020**, 8, 788–798.

[20] A. Barh, L. Høgstedt, P. Tidemand-Lichtenberg, C. Pedersen, presented at CLEO, San Jose, USA (May **2018**).

[21] A. Barh, P. Tidemand-Lichtenberg, C. Pedersen, presented at CLEO/Europe-EQEC, Munich, Germany (June **2019**).

[22] P. Tidemand-Lichtenberg, J. S. Dam, H. V. Andersen, L. Høgstedt, C. Pedersen, *J. Opt. Soc. Am. B* **2016**, 33, D28–D35.

[23] C. Pedersen, Q. Hu, L. Høgstedt, P. Tidemand-Lichtenberg, J. S. Dam, *Opt. Express* **2014**, 22, 28027–28036.

[24] A. Barh, P. J. Rodrigo, L. Meng, C. Pedersen, P. Tidemand-Lichtenberg, *Adv. Opt. Photon.* **2019**, 11, 952–1019.

[25] B. E. A. Saleh, M. C. Teich, "Nonlinear Optics," in *Fundamentals of Photonics*, 2nd Ed. John Wiley & Sons, New Jersey, USA **2007**.

[26] G. Kirchoff, "On the relation between the radiating and absorbing powers of different bodies for light and heat (translation of a German original). *Phil. Mag. Ser 4* **1860**, 20, 1–21.

[27] M. Antinolo, I. Bravo, E. Jimenez, B. Ballesteros, J. Albaladejo, *J. Phys. Chem. A* **2017**, 121, 8322–8331.

[28] C. G. Roffey, *Photogeneration of reactive species for UV curing*, John Wiley & Sons **1997**.

[29] N. Mozner, U. Salz, *Prog. Polym. Sci.* **2001**, 26, 535–576.

[30] N. S. Allen, Ed, "Photopolymerization and photoimaging science and technology," in *Applied Science*, Elsevier, London and New York **1989**.

[31] A. Bagheri, J. Jin, *ACS Appl. Polym. Mater.* **2019**, 1, 593–611.

[32] A. Ovsianikov, J. Yoo, V. Mironov, *3D Printing and Biofabrication*, Springer, Berlin **2018**.

[33] M. del Rocio Bernal-Zamorano, *PhD Thesis*, Technical University of Denmark, January, **2018**.

[34] L. Meng, L. Høgstedt, P. Tidemand-Lichtenberg, C. Pedersen, P. J. Rodrigo, *Opt. Express* **2017**, 25, 14783–14794.

[35] E. K. Kemsley, L. Zhuo, M. K. Hammouri, R. H. Wilson, *Food Chem.* **1992**, 44, 299–304.

[36] S. Sivakesava, J. Iruayaraj, *Appl. Eng. Agric.* **2000**, 16, 543–550.

[37] A. O. Neto, J. Nandenha, M. H. M. T. Assumpcao, M. Linardi, E. V. Spinacé, E. V., R. F. B. de Souza, *Int. J. Hydrog. Energy* **2013**, 38, 10585–10591.

[38] E. L. Veale, J. Irudayaraj, A. Demirci, *Biotechnol. Prog.* **2007**, 23, 494–500.

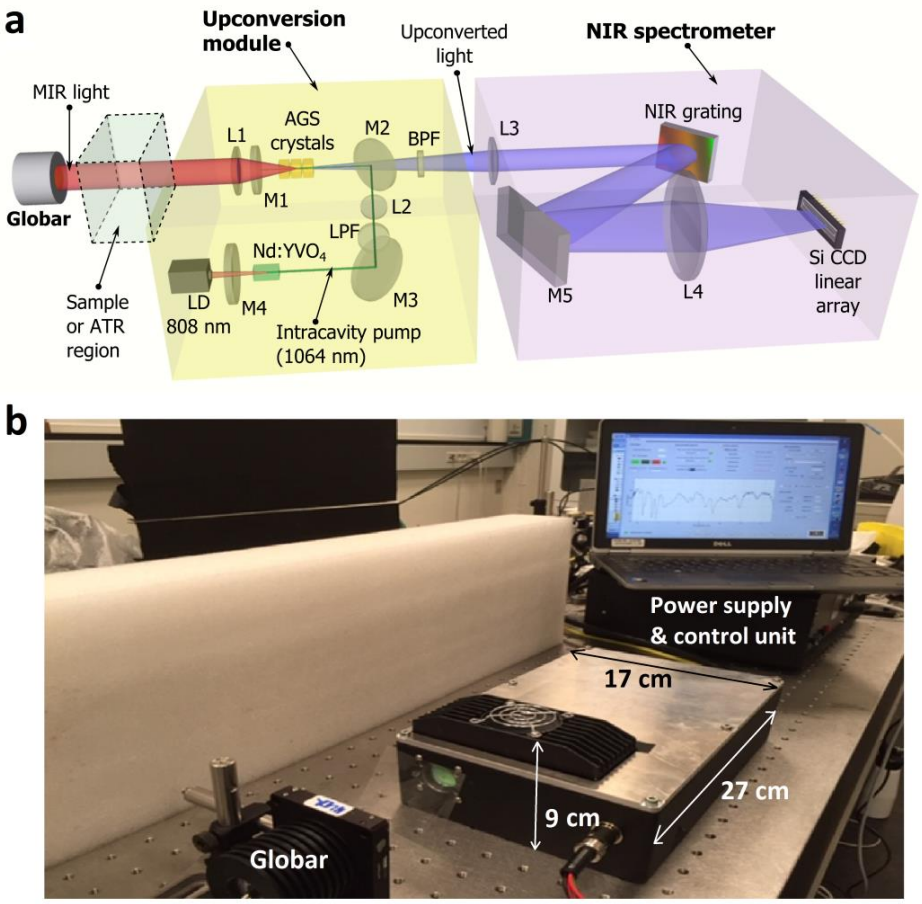

Figure 1. 6-12 µm MIR upconversion spectrometer (MIRUS); (a) Schematic diagram of the 6-12 µm upconversion spectrometer, which consists of an upconversion module, a grating-based NIR spectrometer and a globar as MIR source; (b) Photo of the MIRUS indicating its dimensions.

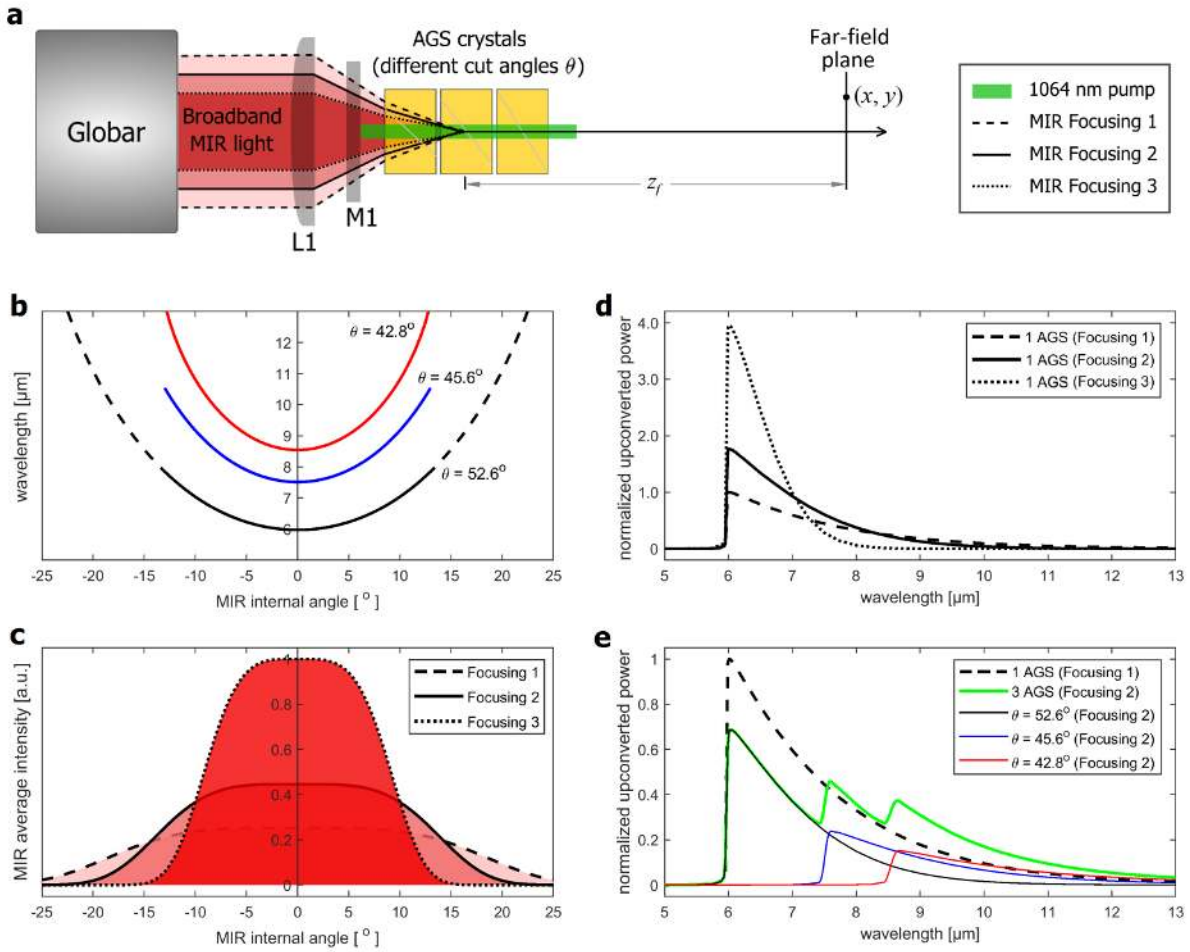

Figure 2. Tailoring the 6-12 μm spectral coverage of MIRUS using a series of $AgGaS_2$ crystals with different cut angles; (a) Illustration of the three $AgGaS_2$ (AGS) crystals with cut angles of 42.8° (left), 45.6° (middle), and 52.6° (right) and a far-field observation plane at an axial distance of z_f from the center of the middle crystal. Three focusing geometries for the MIR light are shown; (b) Phase-match curves of the three crystals showing the optimal internal input angle for every MIR wavelength – i.e., angle that optimizes upconversion efficiency; (c) Models of the brightness profile of the MIR light as a function of angle inside the crystal (relative to the propagation axis of the 1064 nm pump) for the three focusing geometries; (d) Simulated output upconverted power as a function of input wavelength for the single-AGS case for different focusing geometries assuming a blackbody source at 1173 K. (e) Comparison of the upconverted power for cases with single-AGS and three-AGS (both normalized to the peak upconverted power of the former). Focusing geometry 1 is used for the single-AGS and geometry 2 for the three-AGS case.

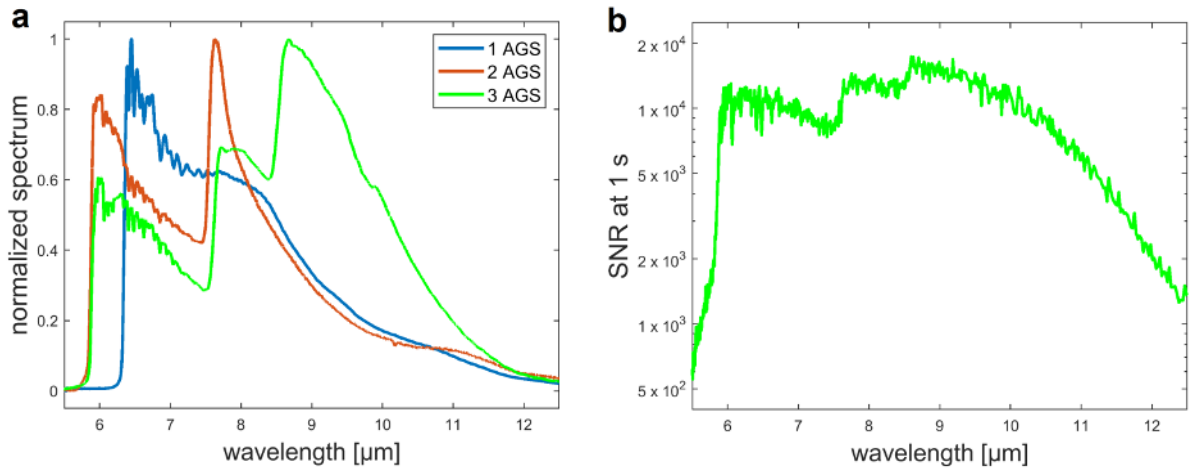

Figure 3. Measured performance of MIRUS; (a) Comparison of the measured MIR spectrum of the SiN globar combined with the spectral response of the instrument in the 6-12 μm range using one, two and three AGS crystals; (b) Measured SNR (at 1 s exposure) of the three-AGS MIRUS exceeding the 10,000 level. For the single-AGS case (1 AGS), the 10-mm long crystal was slightly tilted and therefore had an effective cut angle smaller than 52.6°.

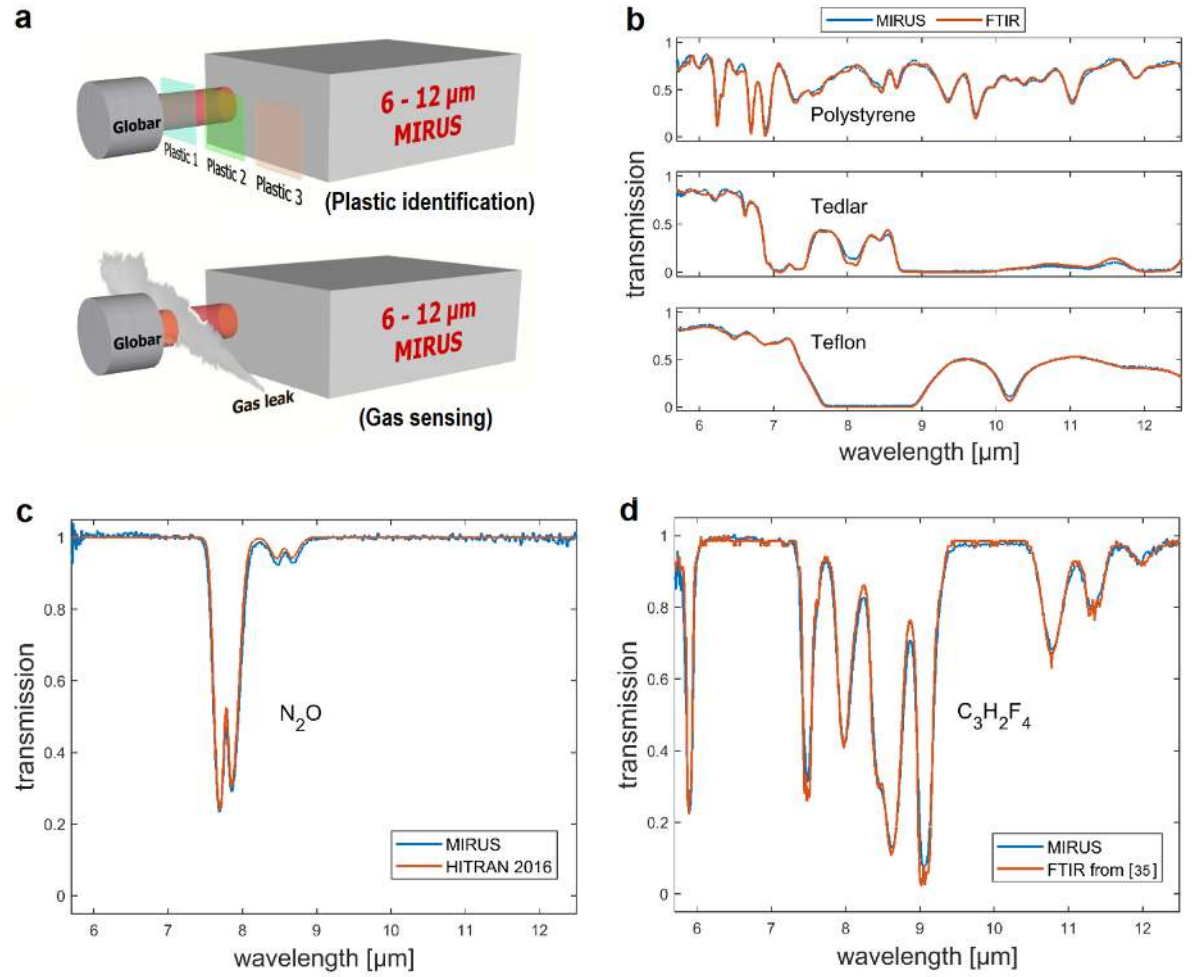

Figure 4. MIRUS as a spectral fingerprint sensor of plastics and gases; (a) Setup using MIRUS for spectroscopy of solid (plastic sheets) and gas samples. (b) Transmission spectra of polystyrene, tedlar, and teflon sheets; (c) Transmission spectrum of nitrous oxide; (d) Transmission spectrum of tetrafluoropropene. All spectra obtained using MIRUS were taken at 11 ms exposure. Each FTIR spectrum in (b) used a few seconds of scan at 8 cm^{-1} resolution.

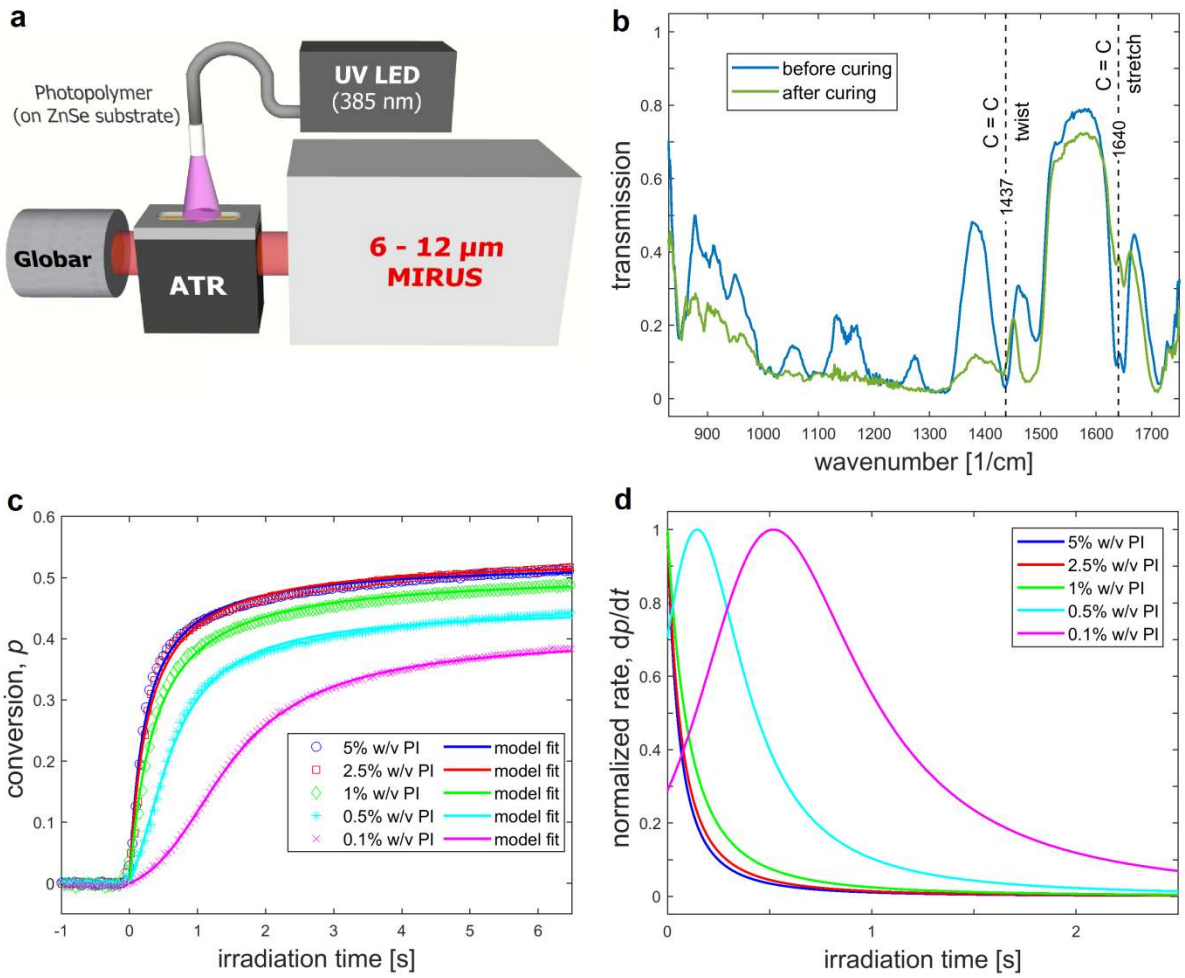

Figure 5. MIRUS-ATR for monitoring fast photopolymerization process in real time; (a) Setup using MIRUS in combination with an ATR for spectroscopic analysis of liquid monomer-oligomer-photoinitiator mixtures; (b) Spectra before and after applying 385 nm UV illumination; (c) Photopolymer conversion *p* (based on the absorption band centered at 1640 cm^{-1}) versus UV irradiation time for various photoinitiator (PI) concentrations derived from the spectra obtained using MIRUS; (d) Corresponding normalized conversion rates.

Table 1. Comparison of MIRUS and the two types of FTIR – three spectrometers used in the MIR fingerprint region using globar illumination.

Parameter	**MIRUS**	FTIR (temporal)	FTIR (spatial)
Detector type	**Si**	HgCdTe	HgCdTe
Requires detector cooling?	**No**	Yes[c)]	Yes[e)]
Requires moving parts?	**No**	Yes	No
Spectral range [cm^{-1}]	**830 – 1750**	350 – 7800	800 – 4000
Spectral resolution [cm^{-1}]	**6**[a)]	0.09, 2, 4, 8, 16	4
Measurement rate [spectra s^{-1}]	**40**[b)]	22.5[d)] at 4 cm^{-1}	0.5
SNR at 1 s	**> 10,000**	~6,000[d)] at 4 cm^{-1}	1,400

[a)] Better spectral resolution is possible using a higher spectral resolution NIR spectrometer module and a ring cavity narrow-linewidth 1064 nm pump; [b)] Faster measurement rates can be achieved by replacing the current CCD linear array detector with a CMOS sensor; [c)] A cryogenic cooling system using LN_2 is used, e.g., in Thermo Scientific Nicolet iS50R; [d)] A tradeoff exists between spectral resolution, SNR and measurement speed of FTIR (temporal) systems. To achieve higher measurement speed, a shorter scan of the movable mirror is used. The rate of 22.5 spectra s^{-1} and SNR at 1 s of ~6,000 at 4 cm^{-1} are estimated from the published specifications for Thermo Scientific Nicolet iS50R (90 spectra s^{-1} at 16 cm^{-1} and SNR at 5 s of 13,000 at 4 cm^{-1}); [e)] Using thermoelectric detector cooling (e.g., Keit IRmadillo and Mettler Toledo ReactIR 702L), instrument sensitivity is low (SNR ~ 1400 at 1 s for Keit IRmadillo). Sensitivity can be improved if LN_2-cooled HgCdTe detector is used (e.g., ReactIR 701L, LN2; SNR data unavailable).

Table of contents entry:

A mid-infrared upconversion spectrometer (MIRUS) with no cryogenically cooled detector or any moving part is presented. The MIRUS operates in the highly relevant 6-12 µm fingerprint region. Combining these attractive features with its high SNR > 10,000 at 6 cm^{-1} resolution and 1 s integration time, the MIRUS could serve as a strong alternative to FTIR spectrometers extensively used in MIR spectroscopy.

Peter John Rodrigo*, Lasse Høgstedt, Søren Michael Mørk Friis, Lars René Lindvold, Peter Tidemand-Lichtenberg and Christian Pedersen

Room-temperature, high-SNR upconversion spectrometer in the 6-12 µm region

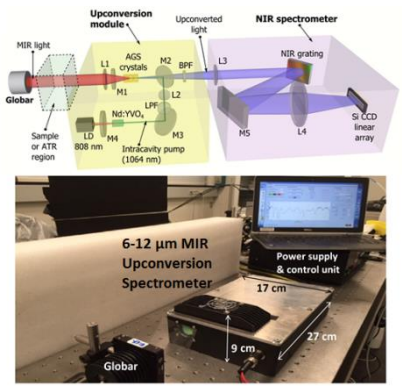

ToC figure

Click here to access/download

Supporting Information

LPR_6-12micron_MIRUS_SupplementaryInfo.docx

Supplementary Video File

Click here to access/download

Supporting Information

LPR_6-12micron_MIRUS_Movie_V1.mp4

8 October 2020

Dear Editor(s) of Laser & Photonics Reviews,

We would like to submit our article with title "*Room-temperature, high-SNR upconversion spectrometer in the 6-12 µm region*" for your consideration in *Laser & Photonics Reviews (LPR).*

As a promising alternative to Fourier Transform Infrared (FTIR) spectrometers that heavily rely on cryogenically cooled detectors, we demonstrate a mid-infrared upconversion spectrometer (MIRUS) that features room-temperature operation, record-high signal-to-noise ratio (>10,000 at 1 second spectral sampling time), no moving parts, and spectral coverage spanning 6 – 12 µm of the spectral fingerprint region. To our knowledge, this is the broadest spectral coverage achieved by an upconversion spectrometer thus far.

In this Article, we present a novel upconversion spectrometer based on stacked $AgGaS_2$ nonlinear crystals with different cut angles that enables MIRUS to achieve the abovementioned features. Furthermore, we highlight the utility of the MIR upconversion spectrometer by demonstrating a few example applications including gas spectroscopy, plastic identification, and real-time monitoring of the kinetics of fast-curing photopolymers. We believe that MIRUS, having advantages over the present gold standard (i.e., FTIR), can open doors in many other applications where fast chemical kinetics can be probed by means of spectroscopy in the MIR fingerprint region.

All authors have contributed to the manuscript and agree with its submission to *LPR*. The work has not been published or submitted (either completely or in part, or in any other form or language) for publication elsewhere. In the manuscript, we also include a conflict of interest declaration.

Yours sincerely,

Peter John Rodrigo
Corresponding Author

DTU Fotonik
Department of Photonics Engineering
Technical University of Denmark
Frederiksborgvej 399
4000 Roskilde
Denmark
E-mail: pejr@fotonik.dtu.dk